Evaluation of Recoverable Hydrocarbon Reserves and Area Selection Methods for In-Situ Conversion of Shale

Lianhua Hou *, Zhongying Zhao *, Xia Luo, Jingkui Mi, Zhenglian Pang, Lijun Zhang, Senhu Lin

Posted Date: 6 May 2024

doi: 10.20944/preprints202405.0272.v1

Keywords: Immature to low-moderate maturity shale; In-situ conversion; Recoverable hydrocarbon reserves; Thermal simulation experiment; Nenjiang Formation in the Songliao Basin

Article

Evaluation of Recoverable Hydrocarbon Reserves and Area Selection Methods for In-Situ Conversion of Shale

Lianhua Hou *, Zhongying Zhao *, Xia Luo, Jingkui Mi, Zhenglian Pang, Lijun Zhang and Senhu Lin

Research Institute of Petroleum Exploration & Development, PetroChina, Beijing 100083, China
* Correspondence: houlh@petrochina.com.cn (L.H.); zhaozhongying@petrochina.com.cn (Z.Z.)

Abstract: It's well known that existing horizontal well drilling and hydraulic fracturing technology that is used to achieve large-scale cost-effective production from immature to low-moderate maturity continental shale in China, where the organic matter mainly exists in the solid form is fairly ineffective. To overcome the obstacles, in-situ conversion technology seems feasible, while implementing it in the target layer along with estimating the amount of expected recoverable hydrocarbon in such shale formations seems difficult. This is because there is no guideline to choose the most appropriate method and select relevant key parameters for this purpose. Hence, based on thermal simulation experiments during the in-situ conversion of crude oil from the Triassic Chang 7_3 Formation in the Ordos Basin and the Cretaceous Nenjiang Formation in the Songliao Basin, this deficiency in knowledge was addressed. First, relationships between the in-situ converted total organic carbon (TOC) content and the vitrinite reflectance (*Ro*) of the shales and between the residual oil volume and the hydrocarbon yield was established. Second, the yields of residual oil and in-situ converted hydrocarbon were measured, revealing their sensitivity to fluid pressure and crude oil density. In addition, a model was proposed to estimate the amount of in-situ converted hydrocarbon based on the TOC, hydrocarbon generation potential, *Ro*, residual oil volume, fluid pressure, and crude oil density. Finally, a method was established to determine key parameters on the final hydrocarbon yield from immature to low-moderate maturity organic material during in-situ conversion in shales. Following the procedure outlined in this paper, estimated recoverable in-situ converted oil in the shales of the Nenjiang Formation in the Songliao Basin was estimated to be approximately 292×10^8 tons, along with 18.5×10^{12} cubic meters of natural gas, in an area of approximately 8×10^4 square kilometers. Collectively, the method developed in this study is independent from the organic matter type and other geological and/or petrophysical properties of the formation and can be applied to other areas globally where there isn't any available in-situ conversion thermal simulation experimental data.

Keywords: immature to low-moderate maturity shale; in-situ conversion; recoverable hydrocarbon reserves; thermal simulation experiment; Nenjiang Formation in the Songliao Basin

1. Introduction

Shale oil has become an important source of energy in the exploitation of global hydrocarbon reserves [1–4]. The most developed continental shale in China is mainly distributed in northern areas such as the Ordos, Songliao, Bohai Bay, and Junggar basins, which cover an area of approximately 400,000 square kilometers, with 200,000 square kilometers of it comprised of layers containing ultra-rich organic matter (TOC > 4 wt.%) and *Ro* values less than 1.0% [5–8]. China has focused geological studies on shale oil since 2010, especially on key technological breakthroughs and exploration dimensions [9–12]. Moreover in 2023, there were over 2500 horizontal wells and the shale oil yield reached 342×10^4 t. However, global shale oil exploration and development practices have revealed

 doi:10.20944/preprints202405.0272.v1

that the existing horizontal well and hydraulic fracturing techniques are not able to achieve cost-effective development of immature to low-moderate maturity shale hydrocarbon reserves [13–17]. Herein, main reasons are the low maturity of the organic matter in such shale layers, low hydrocarbon conversion rate of the convertible organic matter, undeveloped organic pores, poor reservoir connectivity, and a low gas-oil ratio (GOR). Therefore, new technologies should be developed for extraction of hydrocarbons, particularly from immature to low-moderate maturity shales.

Hubbert proposed a peak oil production theory in 1956 which led many countries and companies to target immature to low-moderate maturity shale oil to increase hydrocarbon production [18]. In this respect, a number of international oil companies such as Shell, ExxonMobil, and Total have initiated research on the in-situ conversion of shale oil and have conducted field experiments on various in-situ conversion techniques [14,15,19,20]. In addition, the in-situ electrical heating conversion technology that was proposed by Shell is the most prominent technique to date, since 1960s. They believe that the electrical heating in-situ conversion technology is the preferred method, based on a number of field trials that have been successfully conducted [8–10]. Moreover, in comparison to other existing technologies for this purpose, this technology has been confirmed to be the most feasible option for hydrocarbon extraction from immature to low-moderate maturity shales.

In-situ conversion can be considered to be a physicochemical process in which underground heating of shale facilitates the rapid conversion of convertible solid organic matter and residual oil into light oil and natural gas, leaving the coke and other remaining residues underground. In-situ conversion technology has four main advantages: nearly 100% conversion rate of convertible organic matter into hydrocarbons, a hydrocarbon recovery rate of greater than 60%, light oil production (crude oil gravity of 35–49°API), and the ability to achieve clean extraction and minimize damage to the environment [10].

The basis of a cost-effective development of such technology can be considered as accurately estimating the recoverable hydrocarbon reserves through the in-situ conversion of shales and the selection of suitable areas [17]. Based on the results of thermal simulation experiments on the 7_3 shale in the Triassic Yanchang Formation in the Ordos Basin, in this study, we established an evaluation and area selection method for in-situ conversion of the hydrocarbon yield based on the total organic carbon (TOC) content and vitrinite reflectance (R_o) and assessed the recoverable hydrocarbon reserves in the study area. However, the amount of yield and oil-gas ratios from converted organic material could vary due to the difference in the types of organic matter and the hydrocarbon generation potential of them in different basins, regions, and strata. In addition, the existing methods for the evaluation of recoverable hydrocarbon do not consider these factors, so they are only applicable to areas where thermal simulation experiments have been conducted and relevant models have been established. The uncertainties in the evaluation of recoverable resources can be significant if the existing methods are used in areas where thermal simulation experiments have not been conducted or where there are significant variations in the organic matter types in the shale samples that have been used to conduct such simulations. Therefore, these models might not be necessarily universal and applicable to all areas.

In order to establish a model that is universal for assessing the recoverable hydrocarbon through in-situ conversion of immature to low-moderate maturity shales, in-situ conversion thermal simulation experiment results for the 7_3 shales in the Triassic Yanchang Formation in the Ordos Basin and the Cretaceous Nenjiang Formation in the Songliao Basin were utilized. This model is based on the TOC content, vitrinite reflectance (R_o), hydrocarbon generation potential, residual hydrocarbon volume, and fluid pressure, thus, it can be applied to most areas and provides a reliable guideline for estimating the recoverable hydrocarbon through in-situ conversion of immature to low-moderate maturity shales. According to the shale distribution in the global scale and related parameters, the estimated global recoverable oil reserves through the in-situ conversion of immature to low-medium maturity shale should be approximately 1.4×10^{12} tons, and the estimated global recoverable natural gas resources approximately 1.1×10^{15} cubic meters. The estimated recoverable oil resources in China exceeds 7×10^{10} tons, and the estimated recoverable natural gas resources is more than 6.5×10^{13} cubic

 doi:10.20944/preprints202405.0272.v1

meters. Finally, a criterion is proposed based on the results from the Nenjiang Formation in the Songliao Basin as an example for the selection of the best target layer.

2. Samples and Experimental Methods

The recoverable hydrocarbons from in-situ conversion of immature to low-moderate maturity shale include hydrocarbons generated via thermal decomposition of convertible organic matter, hydrocarbons generated via thermal decomposition of the residual oil in the shale, and the natural gas retained in the shale. In this study, we established a method for evaluating the amount of recoverable hydrocarbon based on in-situ thermal simulation and conversion of material experiments.

2.1. Samples

The samples used in the in-situ conversion thermal simulation experiments conducted in this study are both bulk shale and crude oil.

2.1.1. Shale Samples

The shale samples were collected from the Triassic Yanchang Formation 7_3 in the Ordos Basin and the Cretaceous Nenjiang Formation in the Songliao Basin. Detailed information about the samples is presented in Table 1, and details regarding the procedures in measuring these values can be found in our previous paper [21]. The shale samples of the Nenjiang Formation were collected near Nongan area, which is in the southern part of the Songliao Basin (Figure 1). The burial depths of the samples were 233 to 246 m, and five shale samples with different TOC contents were selected for the experiments. The samples were crushed to 40 to 60 mesh, and then, the selected samples were mixed thoroughly and were separated into several portions. The detailed information about the crushed samples is summarized in Table 2 following the methods previously used on samples in Table 1.

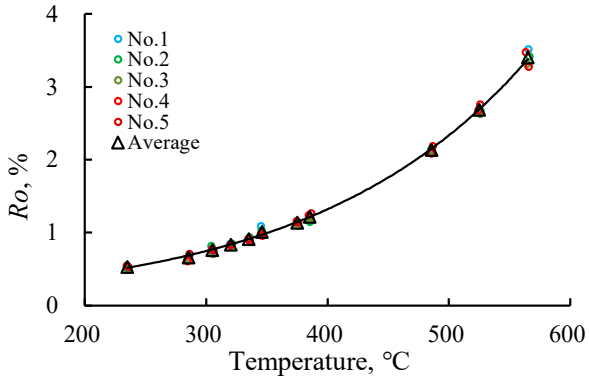

Figure 1. Correlation between pyrolysis temperature and *Ro*.

Table 1. Basic geochemical data of the original unheated shale samples of Chang7_3 formation in Ordos Basin.

Samples Number	No.1	No.2	No.3	No.4	No.5	No.6	No.7	No.8	No.9
TOC, wt.%	0.51	2.03	3.50	5.03	6.44	8.51	13.34	20.67	25.99
S2, mg/g rock	1.99	8.60	17.28	24.53	32.06	42.42	67.17	111.95	138.20
Tmax, ºC	435	433	429	432	431	433	429	428	427
HI, mg/g TOC	388.1	423.0	494.5	487.9	498.2	498.6	503.5	541.5	531.8
Ro, %	0.43	0.46	0.47	0.47	0.47	0.47	0.48	0.47	0.48
Q_{FAOT}, mg/g TOC	1.398	2.02	3.34	3.08	3.42	3.54	3.68	4.22	4.15
Q_{FAGT}, mL/g TOC	0.92	1.19	1.78	1.77	1.81	1.85	1.91	2.08	2.07

 doi:10.20944/preprints202405.0272.v1

Table 2. Basic geochemical data of the original unheated shale samples of Nenjiang formation in Songliao Basin.

Samples Number	No.1	No.2	No.3	No.4	No.5
TOC, wt.%	3.57	6.03	7.69	8.76	11.41
S2, mg/g rock	30.04	51.16	65.68	74.39	97.95
Tmax, ℃	426	426	425	425	424
HI, mg/g TOC	841.34	848.39	854.15	849.25	858.45
Ro, %	0.37	0.37	0.37	0.38	0.38
Q_{FAOT}, mg/g TOC	8.11	8.13	8.14	8.13	8.15
Q_{FAGT}, ml/g TOC	1.93	1.95	1.96	1.95	1.97

2.1.2. Crude Oil Samples

The crude oil samples used the in-situ conversion thermal simulation experiments conducted in this study were collected from five different locations, including the Bohai Bay Basin, Ordos Basin, and Junggar Basin in China. The densities of the liquid oil were 0.85 g/cm^3, 0.87 g/cm^3, 0.92 g/cm^3, 0.95 g/cm^3, and 1.06 g/cm^3.

2.2. Experimental Setup and Procedure

In this study, the experimental setup and procedure used for the thermal simulation experiments on the crude oil and the Nenjiang Formation shale samples were the same as those for the Yanchang Formation 7_3 shale samples that are fully explained in our previous study [21].

2.2.1. Temperature and Thermal Simulation Hydrocarbon Production Experiment

During the thermal simulation experiments, the fluid pressure was set to 5 MPa (725 Psi) and the hydrocarbon venting pressure was set to 7 MPa (1025 Psi). The temperature was increased at a rate of 20°C/d until each preset temperature was reached (first temperature point set as 200°C), and the samples were heated to the preset temperature at a rate of 5°C/d. Then, a constant temperature was maintained for 10 hours. The thermal simulation experiments were conducted on the five shale samples from the Nenjiang Formation in the Songliao Basin. The residual TOC, R_O, and hydrocarbon yield are reported in Table 3.

Table 3. Oil and gas yield, temperature and Ro characteristics of samples after pyrolysis experiments of Nenjiang formation in Songliao basin.

Pyrolysis Temperature,℃	Sample number																		Average T, ℃	Average *Ro*, %
	No.1				No.2				No.3				No.4				No.5					
	T,℃	*Ro*, %	Q_{oil}	Q_{gas}	T,℃	*Ro*, %	Q_{oil}	Q_{gas}	T,℃	*Ro*, %	Q_{oil}	Q_{gas}	T,℃	*Ro*, %	Q_{oil}	Q_{gas}	T,℃	*Ro*, %	Q_{oil}	Q_{gas}		
25	25.06	0.37	0.00	0.00	24.8	0.37	0.00	0.00	25.6	0.37	0.00	0.01	24.6	0.38	0.00	0.01	25.5	0.38	0.00	0.02	25.1	0.37
215	214.3	0.47	0.08	0.00	214.9	0.48	0.19	0.00	216.4	0.44	0.18	0.01	214.8	0.46	0.11	0.01	213.9	0.46	0.13	0.02	214.9	0.46
235	234.5	0.52	0.45	0.01	235.5	0.50	1.15	0.00	234.3	0.55	1.41	0.06	235.8	0.53	1.02	0.03	234.6	0.55	1.61	0.04	234.9	0.53
285	286.4	0.70	2.30	0.01	284.3	0.63	3.76	0.11	285.7	0.65	5.05	0.07	284.5	0.61	6.66	0.20	286.2	0.71	9.87	0.86	285.4	0.66
305	304.8	0.74	3.88	0.01	304.1	0.82	6.49	0.23	305.6	0.71	8.66	0.33	304.8	0.78	11.02	0.45	306.1	0.76	15.34	1.34	305.1	0.76
320	319.7	0.85	5.63	0.18	321.2	0.85	8.98	0.39	320.3	0.81	12.08	0.52	319.7	0.84	14.55	0.59	320.8	0.84	20.35	1.53	320.3	0.84
335	335.5	0.89	7.66	1.11	334.7	0.92	12.23	0.88	335.7	0.94	16.82	1.36	335.8	0.89	19.29	1.91	334.7	0.92	25.91	2.56	335.3	0.91
345	345.2	1.09	10.00	2.30	345.8	1.03	16.45	4.06	346.6	0.99	21.57	4.58	346.2	0.96	24.97	5.08	345.3	0.99	33.23	7.23	345.8	1.01
375	374.9	1.15	12.86	4.02	375.4	1.14	21.91	7.15	375.4	1.10	28.16	8.42	374.6	1.16	31.89	9.32	375.6	1.14	42.01	12.87	375.2	1.14
385	384.8	1.23	13.40	5.34	385.3	1.15	22.82	9.34	385.8	1.20	29.31	11.45	384.3	1.24	33.19	13.34	386.4	1.27	43.70	17.31	385.3	1.22
485	485.6	2.13	13.43	6.20	485.2	2.14	22.87	10.54	485.9	2.12	29.36	12.74	486.5	2.19	33.26	14.64	485.3	2.09	43.79	18.81	485.7	2.13
525	524.7	2.70	13.43	6.56	526.1	2.67	22.87	11.06	525.6	2.63	29.36	13.40	524.2	2.68	33.26	15.21	525.6	2.76	43.79	19.33	525.2	2.69
565	565.3	3.52	13.43	6.99	566.4	3.42	22.87	11.68	564.3	3.32	29.36	14.02	563.3	3.48	33.26	15.84	565.7	3.28	43.79	20.07	565.0	3.40

T- Pyrolysis temperature, ℃; Q_{oil}-Cumulative yields of oil, mg/g rock; Q_{gas}-Cumulative yields of gas, ml/g rock; *Ro*-Vitrinite reflectance of shale organic matter, %.

doi:10.20944/preprints202405.0272.v1

 doi:10.20944/preprints202405.0272.v1

2.2.2. Fluid Pressure and Thermal Simulation Hydrocarbon Production Experiment

Five fluid pressure levels were set during the experiments: 0 MPa (0 Psi), 0.7 MPa (100 Psi), 1.7 MPa (250 Psi), 3.5 MPa (500 Psi), and 5 MPa (725 Psi). The temperature was increased at a rate of 20°C/d until it reached 200°C, and the samples ware heated to the preset temperature of 425°C at a rate of 5°C/d. Then, the samples were kept at a constant temperature for 10 hours. The original geochemical parameters of the shale samples and the hydrocarbon production from the experiments following different fluid pressure conditions are summarized in Table 4.

Table 4. Basic geochemical data of the original unheated shale samples and oil & gas yield.

Basic geochemical		Pressure, Psi/MPa	Oil yield, mg/g rock	Gas yield, mL/g rock
TOC, wt.%	7.82	0/0	108.34	6.30
S2, mg/g rock	66.77	100/0.7	91.97	8.40
Tmax, ℃	425	250/1.7	64.16	10.34
HI, mg/g TOC	853.78	500/3.5	41.52	12.77
Ro, %	0.37	725/5	33.18	15.87

2.2.3. Crude Oil In-Situ Conversion Thermal Simulation Hydrocarbon Production Experiment

In order to determine the contribution of the residual oil to the hydrocarbon produced during in-situ conversion, first, we heated the shale samples to 800°C and maintained this temperature for 48 hours. Second, the cooled sample residues were extracted using dichloromethane, and the extracted residue was heated at 80°C for 48 hours. Finally, the crude oil was mixed with the residues at a mass of 5 wt.%, and then, the temperature was increased at a rate of 5°C/d while fluid pressure was set to 2 MPa (290 Psi), 5 MPa (725 Psi), and 10 MPa (1450 Psi).

3. Results and Discussion

3.1. Relationship between Temperature and Ro in Thermal Simulation Experiment

The *Ro* values of the shale samples at different thermal simulation temperatures were measured on all samples from the Nenjiang Formation following each step of thermal simulation experiments. It was found that there is a strong positive exponential correlation between *Ro* and the thermal simulation temperature (Figure 1). In addition, a relationship between *Ro* and the temperature (Equation (1)) was established, which is necessary for defining the hydrocarbon generation model.

$$R_o = a_1 \times e^{a_2 T}, \quad (1)$$

where *Ro* is vitrinite reflectance (%); T is the thermal simulation temperature (°C); a_1 and a_2 are empirical coefficients with values of 0.1356 and 5.692×10^{-3}, respectively.

3.2. Method of Evaluating Hydrocarbon Production via In-Situ Conversion of Solid Organic Matter in Shale

The extraction target of in-situ conversion is shale with a certain burial depth and thermal maturity. The organic matter in shale consists of solid organic matter that can be converted into hydrocarbons and retained hydrocarbons, which are transformed into light oil and natural gas and can be extracted during the conversion processes. The amount of extracted light oil and natural gas can be defined as the recoverable hydrocarbon and can also be considered to be the hydrocarbon yield in the thermal simulation experiments. Therefore, the hydrocarbons produced via the in-situ conversion of immature to low-moderate maturity shale include both solid organic matter and the retained hydrocarbons.

 doi:10.20944/preprints202405.0272.v1

3.2.1. Basic Model for Evaluating Hydrocarbon Production via In-Situ Conversion of Solid Organic Matter

The shale samples used in the thermal simulation experiments should have been influenced by the storage period and the crushing method. Due to the complete loss of the retained hydrocarbons in the shale, the hydrocarbon yield obtained in the thermal simulation experiments was considered to be mainly from the solid organic matter. The results of the thermal simulation experiments conducted in this study indicate that the hydrocarbon yield from the in-situ conversion of the solid organic matter in different types of shale was consistent with the variations in *Ro*, that is, the hydrocarbon yield decreased as *Ro* increased. The relationship between *Ro* and the hydrocarbon yield via in-situ conversion of the shale of the Nenjiang Formation is shown in Figure 2, and the relationship between the hydrocarbon produced and *Ro* is shown in Figure 3. For the same *Ro* value, there are differences in the hydrocarbon yield and gas-oil ratio of the shale samples with different TOC contents and organic matter types.

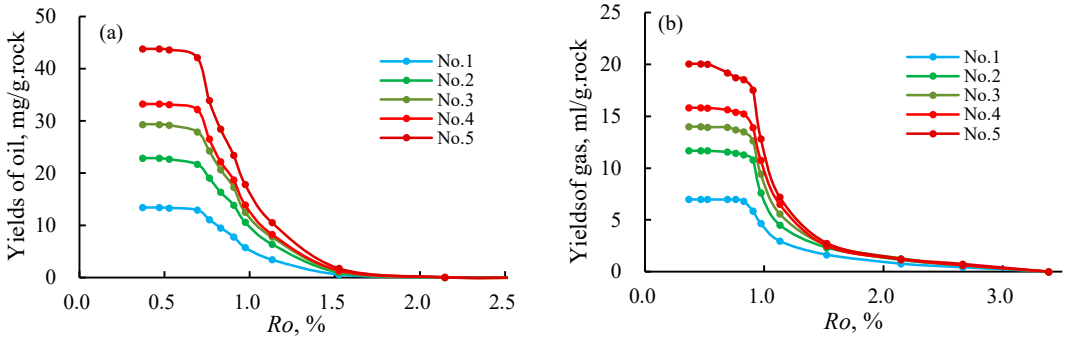

Figure 2. Yield of the remaining hydrocarbons with increasing *Ro*. (a) remaining yield of oil, (b) remaining yield of gas.

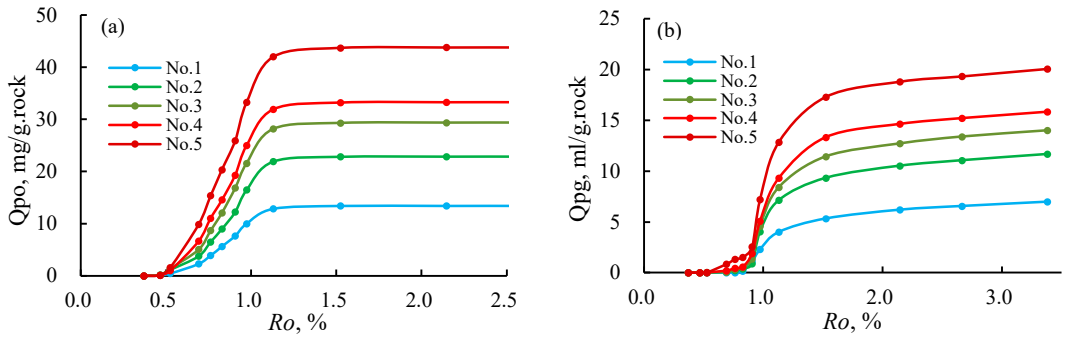

Figure 3. Yields of oil and gas with increasing *Ro*. (a) yield of oil, (b) yield of gas.

Based on the experimental results obtained from 99 different group, from nine shale samples retrieved from the 7_3 shale of the Yanchang Formation in the Ordos Basin, a model for estimating the amount of hydrocarbon yield via the in-situ conversion of solid organic matter based on the TOC and *Ro* was established. Equations (2) and (3), represent the cumulative oil and gas produced, respectively:

$$Q_{po} = b_1 \times \left[\left(b_2 {R_o}^2 + b_3 R_o + b_4\right) TOC + b_5 {R_o}^2 + b_6 R_o + b_7\right], \quad (2)$$

where Q_{po} is the cumulative oil production via in-situ conversion of the solid organic matter (mg/g rock); R_o is the vitrinite reflectance (%); TOC is total organic carbon content (wt.%); and b_1, b_2, b_3, b_4, b_5, b_6, and b_7 are empirical coefficients with values of 2.319, 18.872, −22.784, 6.904, −6.507, 4.303, and −0.632, respectively.

The proposed model for gas production via in-situ conversion of the solid organic matter is as follows:

$$Q_{pg} = b_8 \times \left[\left(b_9 {R_o}^2 + b_{10} R_o + b_{11}\right) TOC + b_{12} ln R_o + b_{13}\right], \quad (3)$$

 doi:10.20944/preprints202405.0272.v1

where Q_{pg} is the cumulative gas production via in-situ conversion of the solid organic matter (mL/g rock); R_o is the vitrinite reflectance (%); TOC is the total organic carbon content (wt.%); and b_8, b_9, b_{10}, b_{11}, b_{12}, and b_{13} are empirical coefficients with values of 1.59231, 1.6821, −1.9765, 0.5819, −0.7199, and −0.3481, respectively.

3.2.2. Method of Correcting Fluid Pressure on the Hydrocarbon Production via In-Situ Conversion

The results of the thermal simulation experiments from the solid organic matter under different fluid pressure conditions suggest that the fluid pressure can control the final hydrocarbon production. Under the same conditions, the oil production decreased and the gas production increased, as the fluid pressure increased (Figure 4); therefore, the impact of fluid pressure has to be considered when evaluating the hydrocarbon production via in-situ conversion of the solid organic matter. Based on the results, a model for correcting the impact of fluid pressure on the hydrocarbon production was developed (Equations (4) and (5)). This model provides a theoretical basis for controlling the bottom-hole pressure of the heating wells, increasing oil production, decreasing gas production, and improving the efficiency of the operation as a whole.

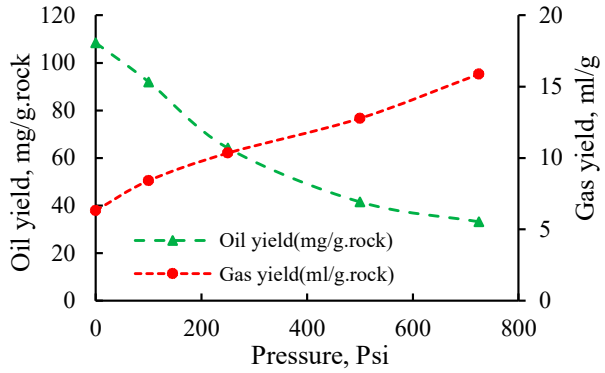

Figure 4. Correlation between oil & gas yield and pressure.

The model for correcting the influence of the fluid pressure on the oil production from the solid organic matter can be expressed as follows:

$$PR_{oil} = c_1 e^{c_2 P}. \quad (4)$$

The model for correcting the influence of the fluid pressure on the gas production from the solid organic matter can be expressed as follows:

$$PR_{gas} = c_3 P + c_4. \quad (5)$$

In these equations PR_{oil} represents the fluid pressure correction coefficient for oil production; PR_{gas} is the fluid pressure correction coefficient for gas production; P is the fluid pressure (MPa); and c_1, c_2, c_3, and c_4 are empirical coefficients with values of 3.1524, −0.2445, 0.1144, and 0.428, respectively.

3.2.3. Method of Correcting Hydrocarbon Generation Potential of Shale

Due to differences in hydrocarbon generation potentials of shale samples containing different types of organic matter, under the same thermal simulation conditions, discrepancies in the amount of hydrocarbon yield during the in-situ conversion process should be expected. Therefore, it is necessary to consider variability of the organic material on the results. Based on the Fischer assay ran on the samples, the amount of hydrocarbon yield from the shale samples with varying thermal maturities, the amount of hydrocarbon yield per unit mass of the total organic carbon content was obtained. This notion is presented in a relationship for the amount of oil, Equation (6), and the amount of gas (Equation (7)) as follows:

$$Q_{FAOT} = d_1 {R_o}^2 + d_2 R_o + d_3, \quad (6)$$

 doi:10.20944/preprints202405.0272.v1

where Q_{FAOT} represents the production per unit mass of total organic carbon content (mg/g.TOC); R_o is the vitrinite reflectance (%); and d_1, d_2, and d_3 are empirical coefficients with values of −11.932, 9.891, and 6.181, respectively.

$$Q_{FAGT} = d_4 {R_o}^2 + d_5 R_o + d_6, \quad (7)$$

where Q_{FAGT} is the gas production per unit volume of total organic carbon content (mL/g TOC); R_o is the vitrinite reflectance (%); and d_4, d_5, and d_6 are empirical coefficients with values of −4.039, 4.641, and 0.707, respectively.

3.2.4. Corrected Model for Evaluating Hydrocarbon Production via In-Situ Conversion of Solid Organic Matter

The model for hydrocarbon production via in-situ conversion of the solid organic matter can be applied in most areas by considering the effects of fluid pressure and different types of organic matter (Equations (8) and (9)) as follows:

$$Q_{poc} = PR_{oil} \times \frac{Q_{FAOT_o}}{Q_{FAOT_{oa}}} \times Q_{po}, \quad (8)$$

where Q_{po} is the uncorrected cumulative oil yield via in-situ conversion of the organic matter (mg/g rock); Q_{poc} is the corrected cumulative oil yield via in-situ conversion of the organic matter (mg/g rock); PR_{oil} is the fluid pressure correction coefficients for oil production; Q_{FAOT_o} is the oil production per unit mass of total organic carbon content in the target layer of shale (mg/g TOC); and $Q_{FAOT_{oa}}$ is the oil production per unit mass of total organic carbon content for the shale sample used in the thermal simulation experiments used to establish the in-situ conversion oil production evaluation model (mg/g TOC). Similar approach can be followed to generate an equation for gas yield as follows:

$$Q_{pgc} = PR_{gas} \times \frac{Q_{FAGT_o}}{Q_{FAGT_{oa}}} Q_{pg}, \quad (9)$$

where Q_{pg} is the uncorrected cumulative gas production via in-situ conversion of the organic matter (mL/g rock); Q_{pgc} is the corrected cumulative gas production via in-situ conversion of the organic matter (mL/g rock); PR_{gas} is the fluid pressure correction coefficients for gas production; Q_{FAGT_o} is the oil production per unit mass of total organic carbon content in the target shale layer (mg/g TOC); $Q_{FAGT_{oa}}$ is the oil production per unit mass of total organic carbon content of the shale sample used in the thermal simulation experiments used to establish the in-situ conversion *model (mg/g TOC).*

3.3. Method of Evaluating the Contribution of the Residual Hydrocarbons to the Hydrocarbon Production via In-Situ Conversion

Residual hydrocarbon exists in immature to low-moderate shales, which contributes to the hydrocarbon production via in-situ conversion. In order to evaluate the contribution of the residual hydrocarbons to the final output, it is necessary to determine the amount of residual hydrocarbon.

3.3.1. Method of Evaluating the Residual Hydrocarbon Reserves

The basic principle of evaluating the contribution of the residual hydrocarbons to the in-situ conversion final product is done by accurately determining its amount. It is difficult to establish a reliable model for evaluating residual hydrocarbons using naturally evolved in shale samples due to the effects of measurement errors and limitations of *Ro* on the distribution of the residual hydrocarbons in the samples. In this study, a model was established using the residual hydrocarbon amounts obtained from the thermal simulation experiments on the shale samples. Moreover, the obtained residual hydrocarbon amounts indicate that the residual oil initially increased and then decreased and the residual gas increased with increasing *Ro* (Figure 5). This model is based on the relationships between the residual hydrocarbon amounts and the TOC and *Ro* (Equations (10) and (11)). In addition, in this study, the target shale layer for in-situ conversion is immature to low-

 doi:10.20944/preprints202405.0272.v1

moderate maturity shale, and the *Ro* values for the samples exposed to thermal simulation are less than 0.9%.

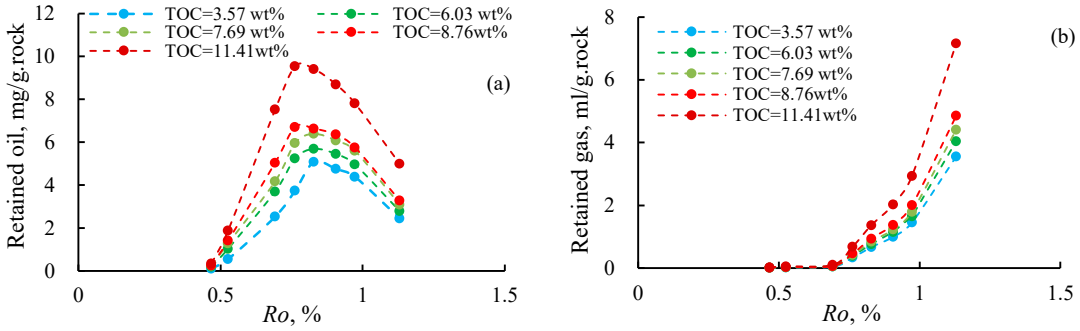

Figure 5. Retained oil and gas with increasing *Ro*. (a) retained oil, (b) retained gas.

The model for assessing the residual oil amount will be:

$$Q_{ro} = \frac{V_s}{V_f} \times \frac{[f_1 e^{(f_2 TOC)} {R_o}^2 + f_3 e^{(f_4 TOC)} R_o + f_5 e^{(f_6 TOC)}]}{\text{TOC}}, \quad (10)$$

where Q_{ro} is the residual oil amount (mg/g rock); TOC is the total organic carbon content (wt.%); R_o is the vitrinite reflectance (%); V_s is the volume of residual oil per unit mass under the pressure and temperature conditions of the thermal simulation experiment (m^3); V_f is the volume of the residual oil per unit mass under the reservoir pressure and temperature conditions (m^3); and f_1, f_2, f_3, f_4, f_5, and f_6 are empirical parameters with values, −54.832, 0.2306, 98.205, 0.2265, −36.58, and 0.2192, respectively.

The model for obtaining the residual gas amount is:

$$Q_{rg} = \frac{V_s}{V_f} \times \frac{f_7 e^{(f_8 TOC)}}{TOC} R_o^{\left(f_9 + \frac{f_{10}}{TOC}\right)}, \quad (11)$$

where Q_{rg} is the residual gas amount (mL/g rock); TOC is the total organic carbon content (wt.%); R_o is the vitrinite reflectance (%); V_s is the volume of residual gas per unit mass under the pressure and temperature conditions of the thermal simulation experiment (m^3); V_f is the volume of residual gas per unit mass under the reservoir pressure and temperature conditions (m^3); and f_7, f_8, f_9, and f_{10} are empirical parameters with values of 2.7565, 0.2312, 6.586, and 2.4555, respectively.

3.3.2. Method of Evaluating the Contribution of the Residual Hydrocarbons to the Hydrocarbon Production via In-Situ Conversion

Due to variations in the properties of the residual oil in shales with different thermal maturity levels, the results of the thermal simulation experiments on shales with different crude oil densities were analyzed as well in this study. The results confirmed the contribution of the residual oil with different properties to the overall hydrocarbon produced during in-situ conversion. Moreover, the thermal simulation experiments conducted in this study revealed that the amount of the hydrocarbon yield are related to the crude oil density and fluid pressure (Figure 6), while the heating rate has a relatively small impact on the total hydrocarbon produced.

 doi:10.20944/preprints202405.0272.v1

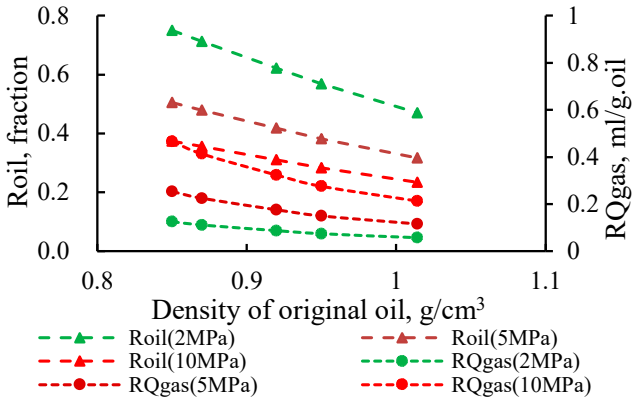

Figure 6. Yield of oil and gas with increasing density of original oil and pressure.

In this study, five crude oil samples were used in the thermal simulation experiments. In addition, a model for obtaining the ratio of oil produced to the original oil consumption during thermal simulation as well as the amount of produced gas per unit mass of the original oil consumption were established.

The model for assessing the ratio of oil produced to the original oil consumed is:

$$R_{oil} = g_1 \times P^{g_2} \times {\rho_o}^{g_3}. \quad (12)$$

The model for obtaining the amount of produced gas per unit mass of the original oil consumed is defined as:

$$RQ_{gas} = g_4 \times P \times {\rho_o}^{g_5} + g_6. \quad (13)$$

In these equations, R_{oil} is the ratio of the oil production to the original oil consumption (mL/g oil); RQ_{gas} is the gas production per unit mass of the original oil consumption (mL/g gas); ρ_o is the oil density during thermal simulation (g/cm³); P is the fluid pressure (MPa); and g_1, g_2, g_3, g_4, g_5, and g_6 are empirical coefficients with values of 0.6645, −0.432, −2.643, 0.02045, −4.44, and 0.0193, respectively.

The amount of residual gas can be considered as the gas produced since there will not be any further cracking of gas during the in-situ conversion process.

3.4. Method of Evaluating Recoverable Hydrocarbon Reserves via In-Situ Conversion of Immature to Low-Moderate Maturity Shale

3.4.1. Model for Evaluating the In-Situ Converted Recoverable Hydrocarbons per Unit Mass of Shale

The final product from the in-situ conversion of immature to low-moderate maturity shale samples consists of three components: hydrocarbons generated via thermal decomposition of the solid convertible organic matter in the shale, the hydrocarbons generated via thermal decomposition of the residual oil in the shale, and natural gas generated via heating of the residual gas in the shale.

The model for measuring the amount of oil produced per unit mass during the in-situ conversion of shale is:

$$Q_{oil} = Q_{poc} + Q_{ro} \times R_{oil}, \quad (14)$$

where Q_{oil} is the recoverable oil per unit mass of shale (mg/g rock); Q_{poc} is the corrected cumulative oil produced via the in-situ conversion of the solid organic matter in the shale (mg/g rock); Q_{ro} is the amount of residual oil per unit mass (mg/g rock); and R_{oil} is the proportion of oil production via in-situ conversion per unit mass of the residual oil.

The model for obtaining the amount of recoverable gas per unit mass under in-situ conversion of shale is:

 doi:10.20944/preprints202405.0272.v1

$$Q_{gas} = Q_{pgc} + Q_{ro} \times RQ_{gas} + Q_{rg,} \quad (15)$$

where Q_{gas} is the recoverable gas amount per unit mass of shale (mL/g rock); Q_{pgc} is the corrected cumulative gas produced as a result of in-situ conversion of the solid organic matter in the shale (mL/g rock); Q_{rg} is the residual gas per unit volume (mL/g rock); Q_{ro} is the residual oil per unit mass (mg/g rock); and RQ_{gas} is the in-situ converted gas per unit volume of residual oil (mL/g oil).

3.4.2. Model for Evaluating the Abundance of In-Situ Converted Recoverable Hydrocarbons

The abundance (quantity in the area under operation) of recoverable hydrocarbon per square kilometer area can be calculated as follows:

$$AOR = 10^{-7} Q_{oil} \times H_{shale} \times \rho_{shale,} \quad (16)$$

$$AGR = 10^{-8} Q_{gas} \times H_{shale} \times \rho_{shale,} \quad (17)$$

where AOR is the abundance of recoverable oil (10^4 t/km^2); AGR is the abundance of recoverable gas (10^8 m^3/km^2); Q_{oil} is the recoverable oil per unit mass of the in-situ converted shale (mg/g rock); Q_{gas} is the recoverable gas per unit volume of the in-situ converted shale (mL/g rock); ρ_{shale} is the density of the shale (g/cm^3); and H_{shale} is the thickness of the in-situ converted shale layer (m).

3.4.3. Method of Determining the Lower Limits of the Recoverable Oil Reserves for In-Situ Conversion

(1) Method for determining the lower limit of the recoverable oil reserves

The minimum rate of return on the investment (IRR_{cut_off}) can be determined using the investment return affordability which infers what return level is affordable or feasible for the investor or operator to fulfil this operation. According to the average values of the fixed investment, operating costs, taxes, reclamation costs, abandonment costs, sunk costs, hydrocarbon sale prices, and commodity rates for a production cycle, the lower limit for the amount of the recoverable oil reserves ($EUR\_BOE_{cut\_off}$) to make the operation economically feasible can be obtained as follows:

$$EUR\_BOE_{cutoff} = \sum_i^n [1 + IRR_{cutoff}]^i \frac{Capex_i + Opex_i + Dct_i + SC_i + Rf_i}{CR_{oil_i}(P_{oil\_i} - Tax_{oil\_i}) + CR_{gas\_i}(P_{gas\_i} - Tax_{gas\_i})}] \quad , (18)$$

where $EUR\_BOE_{cut\_off}$ is the economic lower limit of the amount of recoverable oil (10^4 t), $Capex_i$ represents the average fixed investment for year i ($); $Opex_i$ represents the average operating costs for year i ($); Dct_i represents the average abandonment costs for year i ($); SC_i represents the average sunk costs for year i ($); Rf_i represents the average reclamation costs for year i ($); CR_{oil_i} represents the average commodity rate for oil production for year i; CR_{gas_i} represents the average commodity rate for gas production for year i; P_{oil_i} is the average oil sales price for year i ($/$10^4$ t); P_{gas_i} is the average gas sales price for year i ($/$10^4$ t); Tax_{oil_i} is the average tax per unit oil production for year i ($/$10^4$ t); Tax_{gas_i} is the average tax per unit gas production for year i ($/$10^4$ t); n is the production period (year); and IRR_{cut_off} is the lower limit value of the rate of return on the investment.

(2) Method for determining the lower limit of the recoverable oil reserves per unit mass of rock

The lower limit in the amount of recoverable oil per unit mass of rock can be determined using Equation (19), which is based on the effective heated rock volume, rock density, and the economic lower limit of the amount of recoverable oil:

$$Q_{BOE\_cutoff} = 10^7 \frac{EUR\_BOE_{cutoff}}{V_{rock} \times \rho_{rock}}, \quad (19)$$

where Q_{BOE_cutoff} is the lower limit of the recoverable oil per unit mass of rock (mg/g rock); EUR_BOE_{cutoff} is the economic lower limit of the recoverable oil for a well group (10^4 t); V_{rock} is the effective rock volume heated by a well group (m^3); and ρ_{rock} is the density of the effective heated rock (g/cm^3).

 doi:10.20944/preprints202405.0272.v1

3.4.4. Method of Determining Favorable Layers for In-Situ Conversion

When heating favorable layers during the in-situ conversion process, the average recoverable oil per unit mass of rock must exceed the amount of economic lower limit in order to achieve efficient extraction. This basis can be used to determine the favorable layers for in-situ conversion.

3.4.5. Method of Determining Favorable Areas for In-Situ Conversion

The lower limit in carrying in-situ conversion in shale layers containing immature to low-moderate maturity organic matter can be determined based on developed equations and costs associated with the process. Moreover, areas where the amount of recoverable oil is not less than the quantity of the lower limit threshold, can be defined as favorable areas.

3.5. Evaluation of Recoverable Hydrocarbon Reserves in the Nenjiang Formation in the Songliao Basin

3.5.1. Geologic Background

The Songliao Basin is located in the northeastern part of China. It is bounded by the Greater Hinggan Mountains to the west, the Lesser Hinggan Mountains to the northeast, and the Changbai Mountains to the east [22–24]. Moreover, it is rhomboid-shaped, trends north-northeast, covers an area of 26×10^4 km^2, has a length of 750 km from north to south, and has a width of 350 km from west to east. In addition, it is a large-scale continental rift basin developed in the Cenozoic [23,24]. The Cretaceous Nenjiang Formation can be divided into five sections [25,26], which were deposited in a large-scale lacustrine environment characterized by semi-deep to deep lakes with a subtropical semi-humid climate. Furthermore, the first section was developed in a reducing sedimentary environment in a brackish-slightly brackish lake, and the second section was developed in a reducing depositional environment in a slightly brackish-freshwater lake [27–31]. The organic matter consists of type I-II$_1$ kerogen and is predominantly type I kerogen (Figure 7).

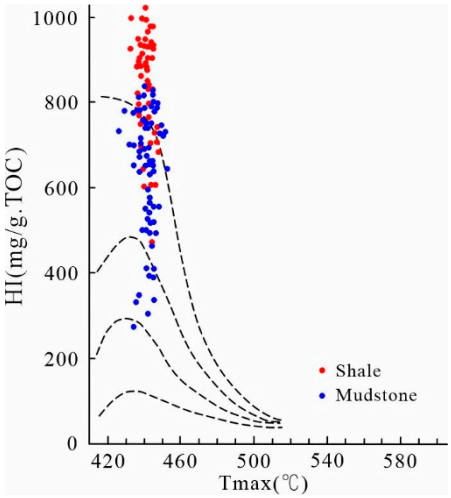

Figure 7. The relationship between HI and Tmax in the shale of Nenjiang Formation.

3.5.2. Key Parameters for In-Situ Conversion

In this study, to determine the key parameters for evaluating the in-situ conversion of hydrocarbon resources and further selection of the area were conducted via core analysis from 151 wells and logging data for 526 wells in the Nenjiang Formation. This is the recommended method for determining the key parameters, such as the TOC, *Ro*, hydrogen index (HI), and shale thickness.

(1) Maturity of organic matter

The organic matter in the Nenjiang Formation is immature to low-moderate maturity, and thus, makes a relatively small contribution to the conventional hydrocarbon accumulation in the Songliao Basin [32]. Moreover, the hydrocarbons generated from the shales of the Nenjiang Formation have

 doi:10.20944/preprints202405.0272.v1

mainly accumulated in the Heidimiao oil reservoir, which has proven petroleum reserves of less than 8000×10^4 tons. The distribution of the *Ro* values determined via core analysis of the Nenjiang Formation samples is limited, and previous studies have focused on local depressions and limited areas, which makes it difficult to meet the requirements for the detailed evaluation of the *Ro* across the entire basin [32–34]. The core *Ro* measured data from 151 wells in the Nenjiang Formation (Figure 8) was utilized in this study. It was found that the *Ro* is positively correlated with the burial depth (Figure 9), hence, a *Ro* prediction model was developed (Equation (20)). In order to verify the reliability of this model, the *Ro* values of shale samples from cores, retrieve from six different wells located outside the experimental area were employed (Figures 8 and 9), and it was found that the relative error between the newly measured *Ro* data and the *Ro* data from the model is less than 9%. This result indicates that our *Ro* prediction model can meet the requirements for the overall evaluation of the Nenjiang Formation. In addition, the logging data from 526 wells were used to calculate the *Ro* in order to obtain its spatial/areal distribution. It was revealed that the main range of the *Ro* is 0.3–0.9%, and the best in-situ conversion occurs when *Ro* is less than 0.9% (Figure 8).

$$Ro = k_1 e^{k_2 D}, \tag{20}$$

where *Ro* is the vitrinite reflectance (%); D is the burial depth (m); and k_1 and k_2 are empirical coefficients with values of 0.2753 and 6.124×10^{-4}, respectively.

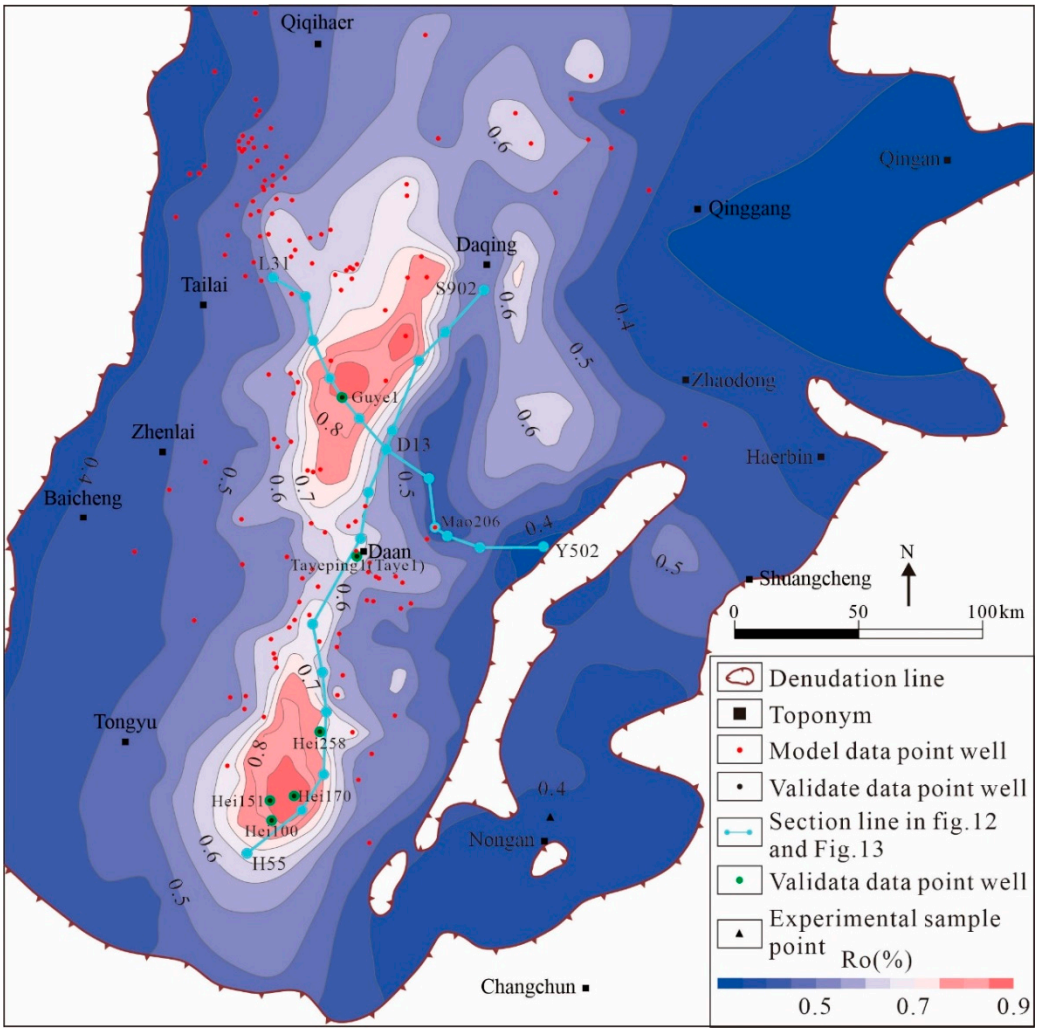

Figure 8. Distribution of R_o in the shale of the Nenjiang Formation in the Songliao Basin.

 doi:10.20944/preprints202405.0272.v1

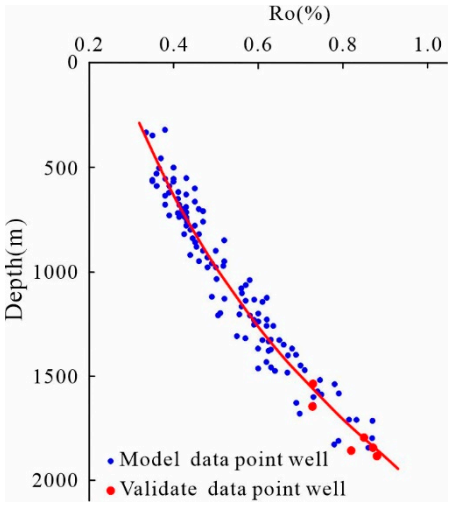

Figure 9. Plot of *Ro* versus burial depth.

(2) Total organic carbon content

The TOC can be considered to be the material input for the in-situ conversion and is an important parameter for evaluating the potential of having economic recoverable hydrocarbon amounts. Based on the analysis of cores from 151 wells and logging data from 526 wells in the Nenjiang Formation, first the core measured data were used to calibrate the logging data, and the overlapping resistivity-sonic method was then employed for prediction of TOC in the entire section [35]. It was understood that the calculated TOC values correspond well with the core measured results (Figure 10), and the relative error between the calculated TOC values and the core analysis measured values is less than 8%, which is in an acceptable range for overall estimation of the TOC where measurements are missing.

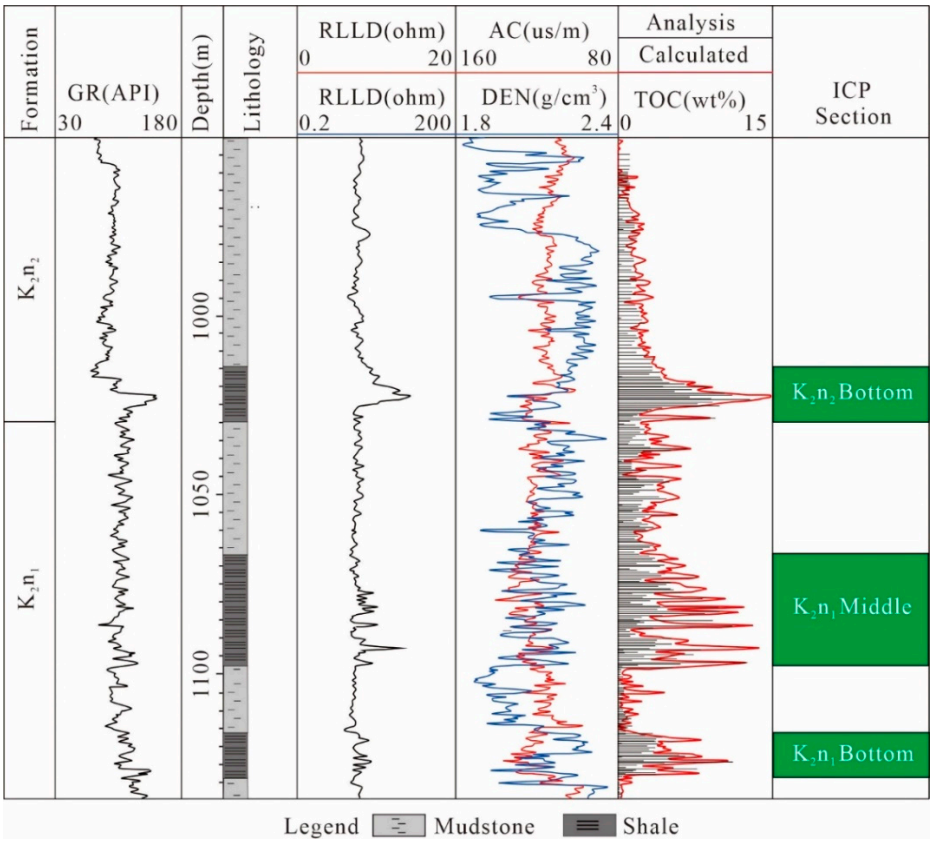

Figure 10. Well log interpretation of TOC in Well M206.

 doi:10.20944/preprints202405.0272.v1

(3) Hydrocarbon generation potential of shale

The potential production of residual hydrocarbon in shale is an important parameter for assessing the overall amount of hydrocarbon yield during in-situ conversion, which can be characterized by the hydrogen index or generated hydrocarbon amounts of the Fischer assay. The experimentally measured hydrogen index and the Fischer assay generated hydrocarbon amounts from the immature shale samples in the Nenjiang Formation exhibit a relatively good linear relationship. Because the Fischer assay is generally a more complicated procedure than pyrolysis which the former provides us the hydrogen index, models defining the relationship between these two parameters were established (Equations (22) and (23)) to correct the in-situ converted hydrocarbon amounts using the Fischer assay.

$$Q_{FAOT} = l_1 HI + l_2, \tag{22}$$

where Q_{FAGT} is the amount of oil generated per unit mas of TOC content (mg/g TOC); *HI* is the hydrogen index (mg/g TOC); and l_1 and l_2 are empirical coefficients with values of 0.00232 and 6.15581, respectively.

$$Q_{FAGT} = l_3 HI + l_4, \tag{23}$$

where Q_{FAOT} is the amount of gas generated per unit volume of TOC content (mL/g TOC); HI is the hydrogen index (mg/g TOC); and l_3 and l_4 are empirical coefficients with values of 0.00232 and −0.02419, respectively.

Furthermore, based on the relationship between the hydrogen index and *Ro* from 151 wells, it was understood that the hydrogen index is positively correlated with the *Ro* (Figure 11), and a model was defined to estimate the HI (Equation (24)). In addition, the HI results were calculated using the *Ro* data for 526 wells in the Nenjiang Formation in order to study the spatial/areal distribution of the HI values in the region.

$$HI = j_1 \ln(R_o) + j_2, \tag{24}$$

where *HI* is the hydrogen index (mg/g TOC); R_o is the vitrinite reflectance (%); and j_1 and j_2 are empirical coefficients with values of −335.498 and 492.571, respectively.

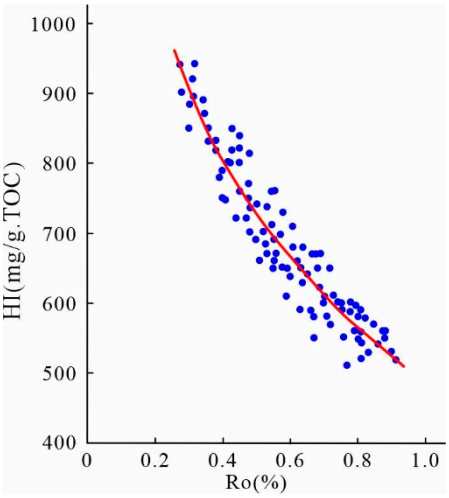

Figure 11. Plot of HI versus R_o.

(4) In-situ conversion of shale layer and thickness

Based on operational constraints and costs associated with in-situ conversion, we can apply the models proposed in this paper for estimating the amount of recoverable hydrocarbon as well as the lower limit value per unit mass of the in-situ converted shale, in order to determine the suitability of this operation in the Nenjiang Formation as the target layer based on its TOC, HI, and *Ro* values. The Nenjiang Formation satisfies the conditions for in-situ conversion, including three separate zones:

 doi:10.20944/preprints202405.0272.v1

the bottom of the Nenjiang Formation II, the middle of the Nenjiang Formation I, and the bottom of the Nenjiang Formation I (Figure 10).

The thickness of these three sections vary considerably in the region. In the east-west direction (Figure 12), the bottom of the Nenjiang Formation I is relatively less present and has the smallest thickness, while the middle of the Nenjiang Formation I is relatively present in the area, with a maximum overall thickness and significant variation in the thickness from east to west. Finally, the bottom of the Nenjiang Formation II is similar to that of the middle of Nenjiang Formation I, but its overall thickness is slightly greater than that of the bottom of the Nenjiang Formation I and is notably less than that of the middle of the Nenjiang Formation I, with a relatively small overall variation in thickness in the east-west direction. In the north-south direction (Figure 13), the bottom of the Nenjiang Formation I has the smallest thickness and the smallest distribution, which is similar to that of in the east-west direction. In contrast, the other two sections exhibit significantly different areal distribution in the east-west direction, and the variation in the thickness of the bottom of the Nenjiang Formation II is the most significant. In terms of the overall thickness, the bottom of the Nenjiang Formation II is close to the middle of the Nenjiang Formation.

In the target layer, the thickness of the bottom of the Nenjiang Formation II ranges from 6 m to 22 m, and the area where the thickness exceeds 15 m is approximately 5,661 km^2 (Figure 14). The TOC values are from 5.5 wt.% to 9.0 wt.%, and the area where the TOC exceeds 6.0 wt.% is approximately 30,154 km^2 (Figure 15). Moreover, the thickness of the bottom of the Nenjiang Formation I varies from 2 to 10 m, while the average TOC value is 5.0–7.5 wt.%, and the area where the TOC exceeds 6.0 wt.% is approximately 6,150 km^2. In addition, considering the middle of the Nenjiang Formation I, the thickness ranges from 8 to 34 m, and the area where the thickness is more than 15 m is approximately 12,506 km^2. The average TOC value in this zone varies from 4.5 wt.% to 6.5 wt.%, with the TOC more than 6.0 wt.% covering approximately 2,264 km^2.

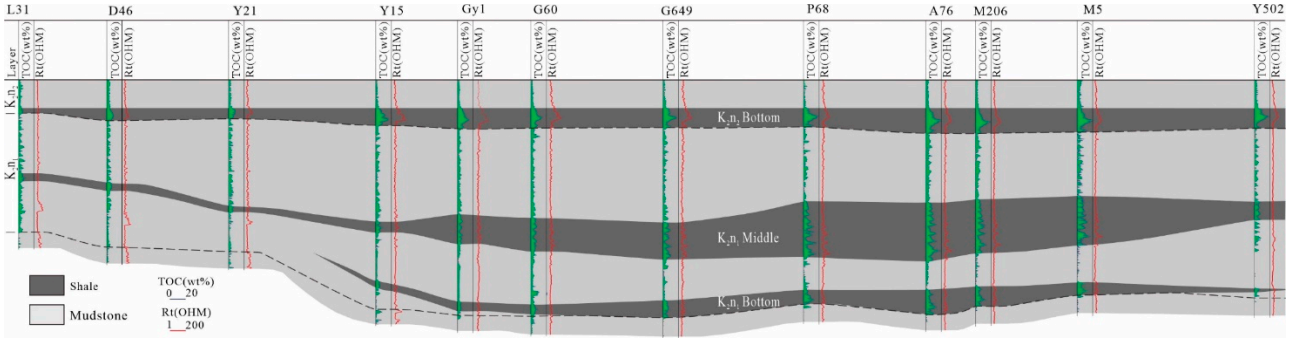

Figure 12. East-west distribution of in-situ converted shale section of Nenjiang Formation.

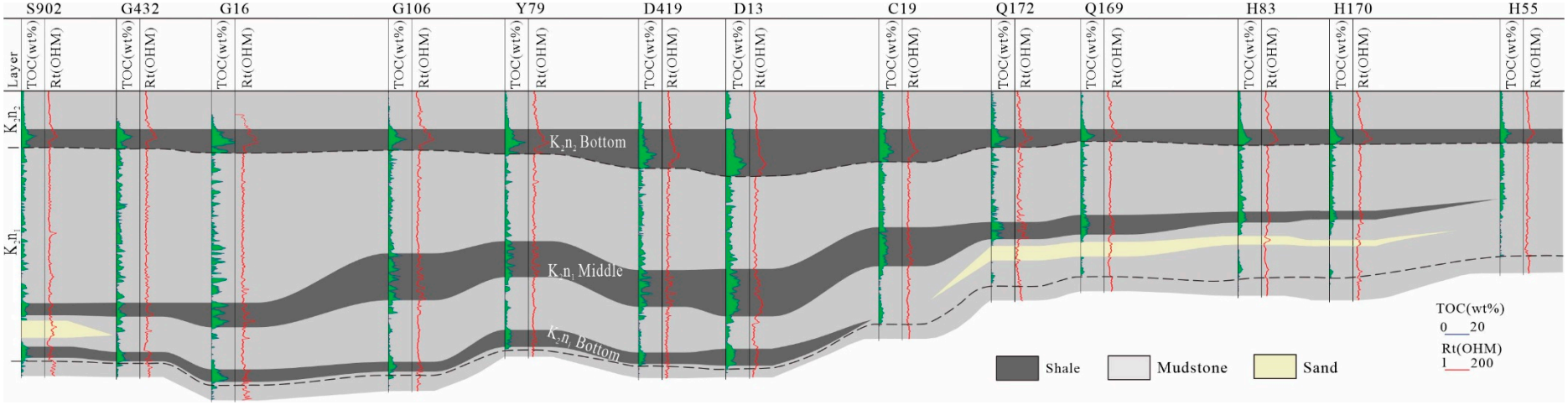

Figure 13. North-south distribution of in-situ converted shale section of Nenjiang Formation.

doi:10.20944/preprints202405.0272.v1

 doi:10.20944/preprints202405.0272.v1

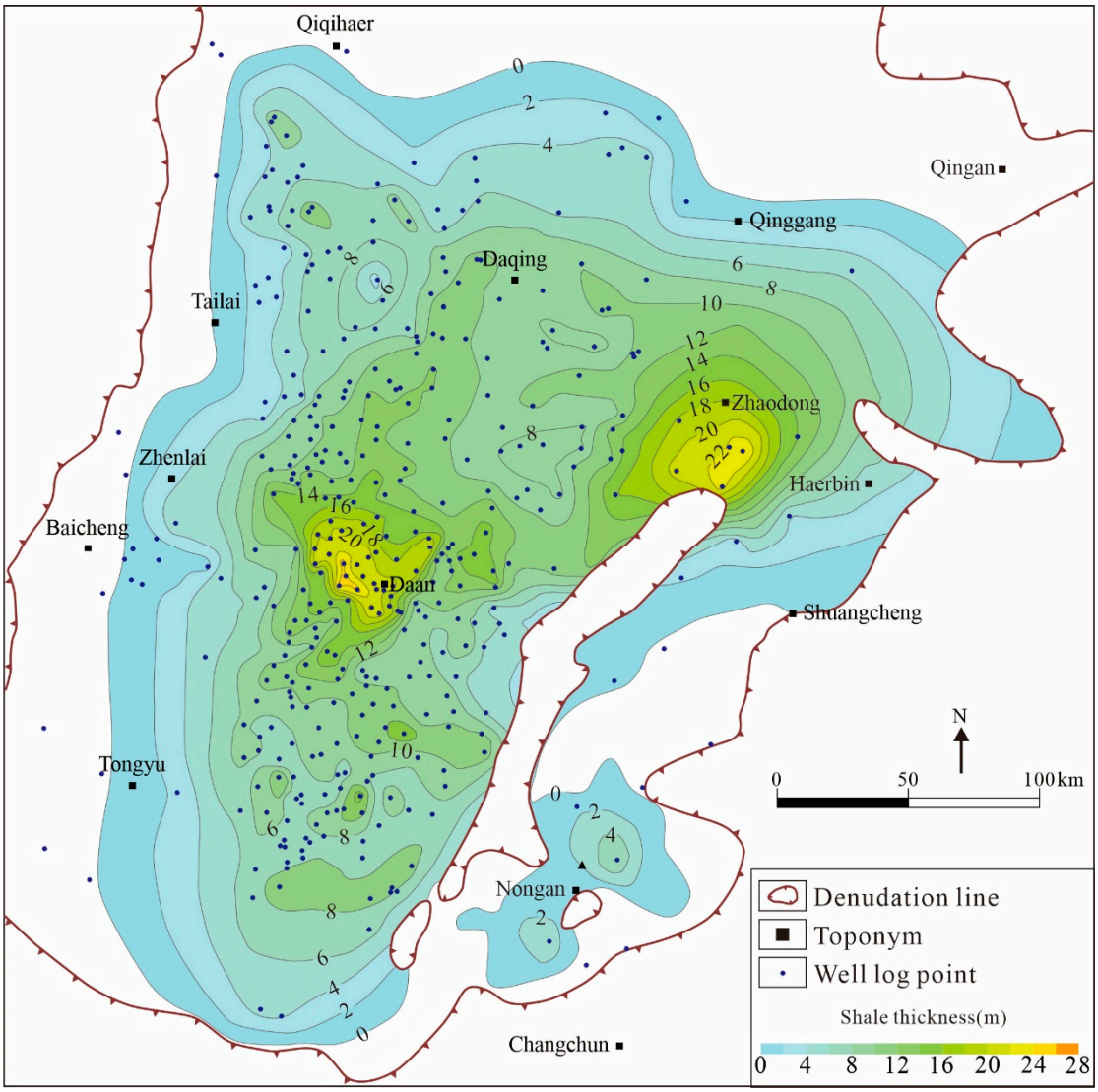

Figure 14. Thickness distribution in the bottom of Nenjiang Formation II.

 doi:10.20944/preprints202405.0272.v1

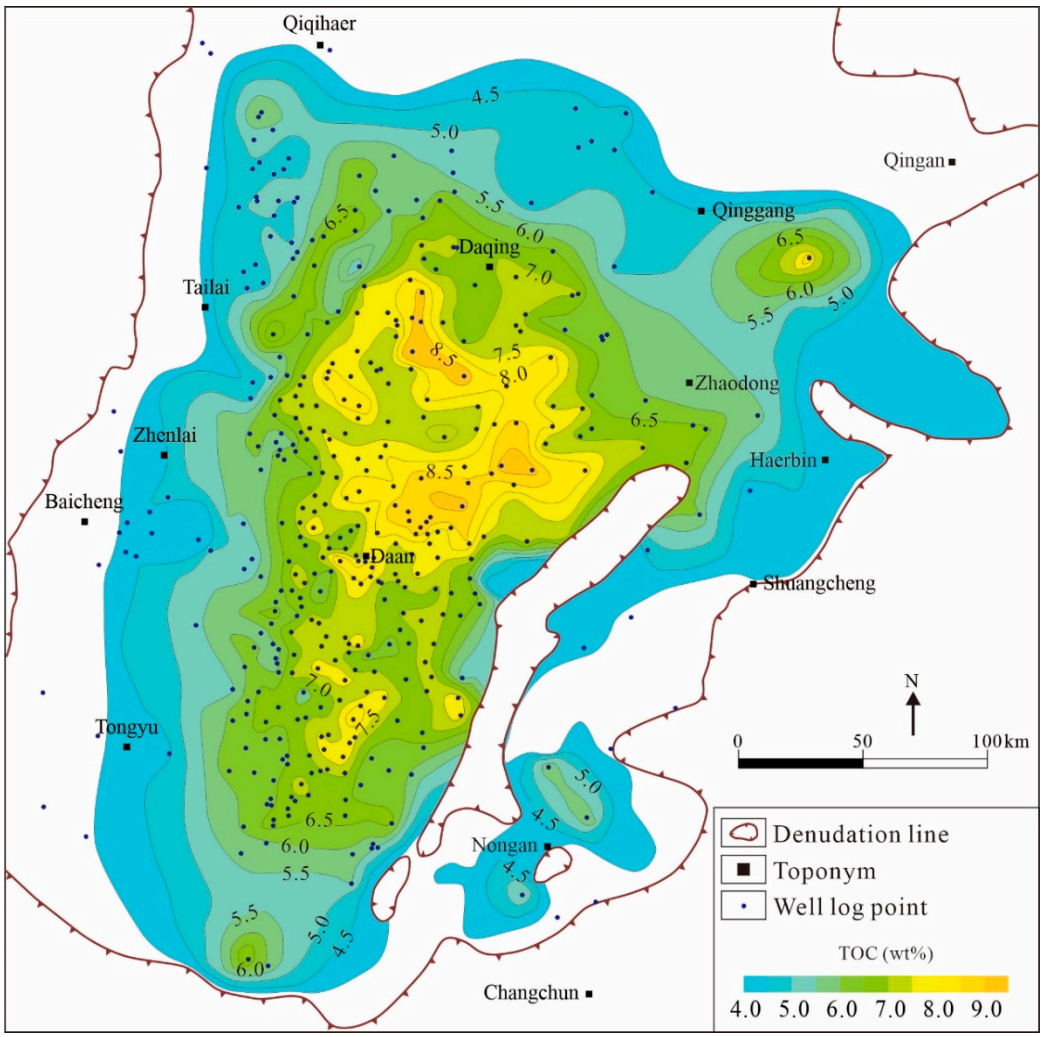

Figure 15. TOC distribution in the bottom of Nenjiang Formation II.

3.5.3. Evaluation of Recoverable Hydrocarbon Reserves

Based on the key parameters of the target layer in the study area, estimation of the amount of recoverable hydrocarbon following in-situ conversion in these three sections was carried out using the methods and steps proposed here.

The results suggest that the amount of recoverable hydrocarbon following in-situ conversion in these three sections would be significant, with approximately 292.02×10^8 t of oil and, natural gas of about 18.58×10^{12} m^3. In particular, the bottom of the Nenjiang Formation II showed approximately 140.85×10^8 t of recoverable oil and approximately 9.22×10^{12} m^3 of recoverable natural gas, and it covers an area of approximately 8.2×10^4 km^2. In addition, the middle of the Nenjiang Formation I showed an approximately 123.82×10^8 t of recoverable oil and about 7.60×10^{12} m^3 of recoverable natural gas, in an area of approximately 7.7×10^4 km^2. The bottom of the Nenjiang Formation I, would produce 27.35×10^8 t of recoverable oil and 1.76×10^{12} m^3 of recoverable natural gas, in an area of approximately 4.4×10^4 km^2 (Table 5).

Table 5. Oil and gas recoverable resources of in-situ converted shale section of Nenjiang Formation in Songliao Basin.

Formation	Oil, 10^8t	Gas, $10^{12}m^3$	Area, km^2
the bottom of Nenjiang Formation II	140.85	9.22	82214

 doi:10.20944/preprints202405.0272.v1

the middle of Nenjiang Formation I	123.82	7.60	77407
the bottom of Nenjiang Formation I	27.35	1.76	44781
Total	292.02	18.58	
Overlap area			82214

The abundance (per unit area) of recoverable oil in the bottom of the Nenjiang Formation II ranges from 20×10^4 t/km^2 to 80×10^4 t/km^2 (Figure 16), with the abundance recoverable natural gas from 1.5×10^8 m^3/km^2 to 4.5×10^8 m^3/km^2 (Figure 17), and oil equivalent from 30×10^4 t/km^2 to 130×10^4 t/km^2 (Figure 18). The abundance of recoverable oil in the middle of the Nenjiang Formation I ranges from 10×10^4 t/km^2 to 80×10^4 t/km^2, with the abundance of recoverable natural gas ranging from 1.0×10^8 m^3/km^2 to 4.5×10^8 m^3/km^2, and oil equivalent that is around 30×10^4 t/km^2 to 120×10^4 t/km^2. The abundance of recoverable oil in the bottom of the Nenjiang Formation I was estimated to be 10×10^4 t/km^2 to 20×10^4 t/km^2, while the abundance of recoverable natural gas would vary from 0.5×10^8 m^3/km^2 to 1.5×10^8 m^3/km^2, and finally, recoverable equivalent oil that is 20×10^4 t/km^2 to 40×10^4 t/km^2.

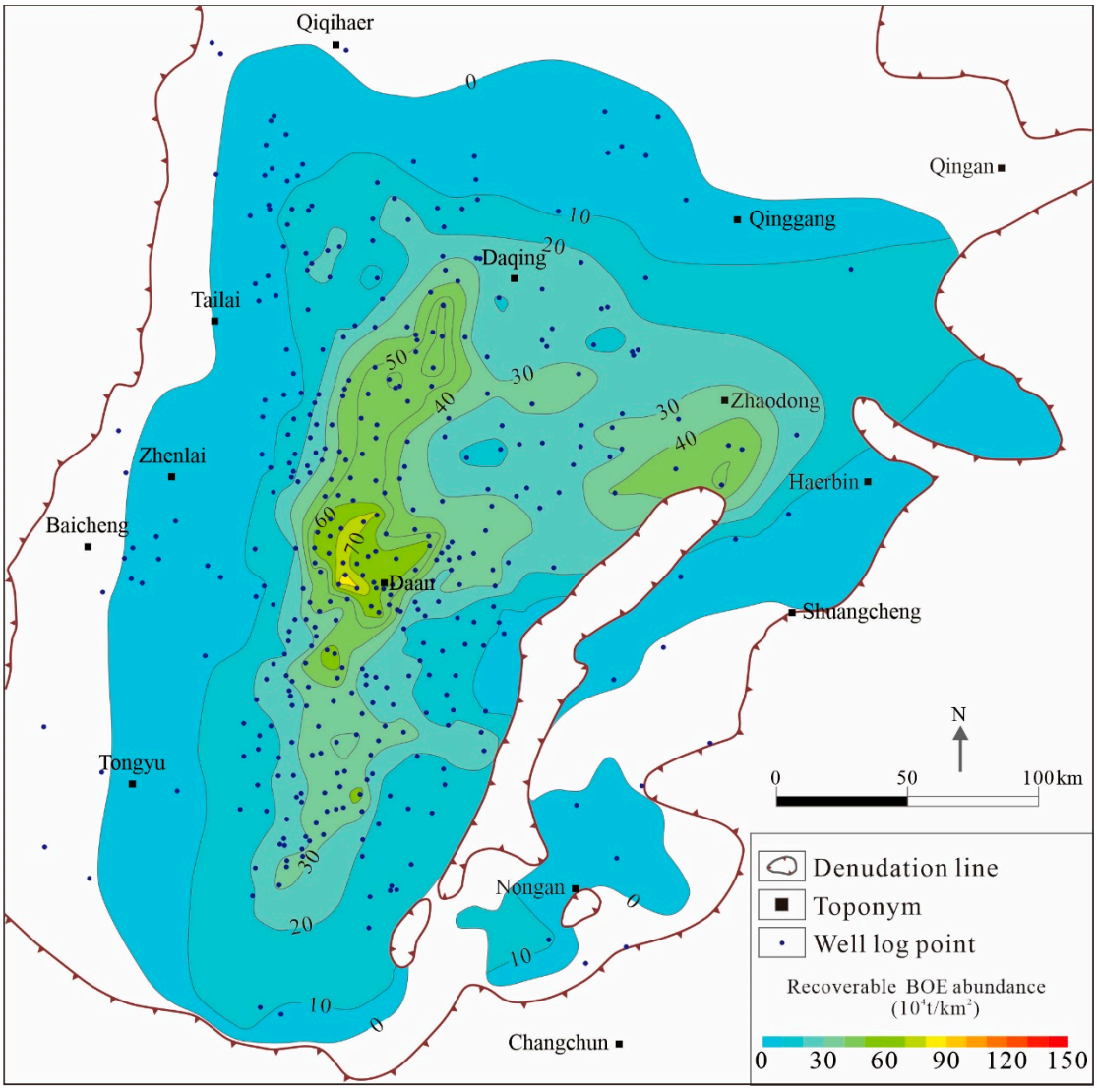

Figure 16. Abundance distribution of recoverable petroleum reserves in the bottom of Nenjiang Formation II.

 doi:10.20944/preprints202405.0272.v1

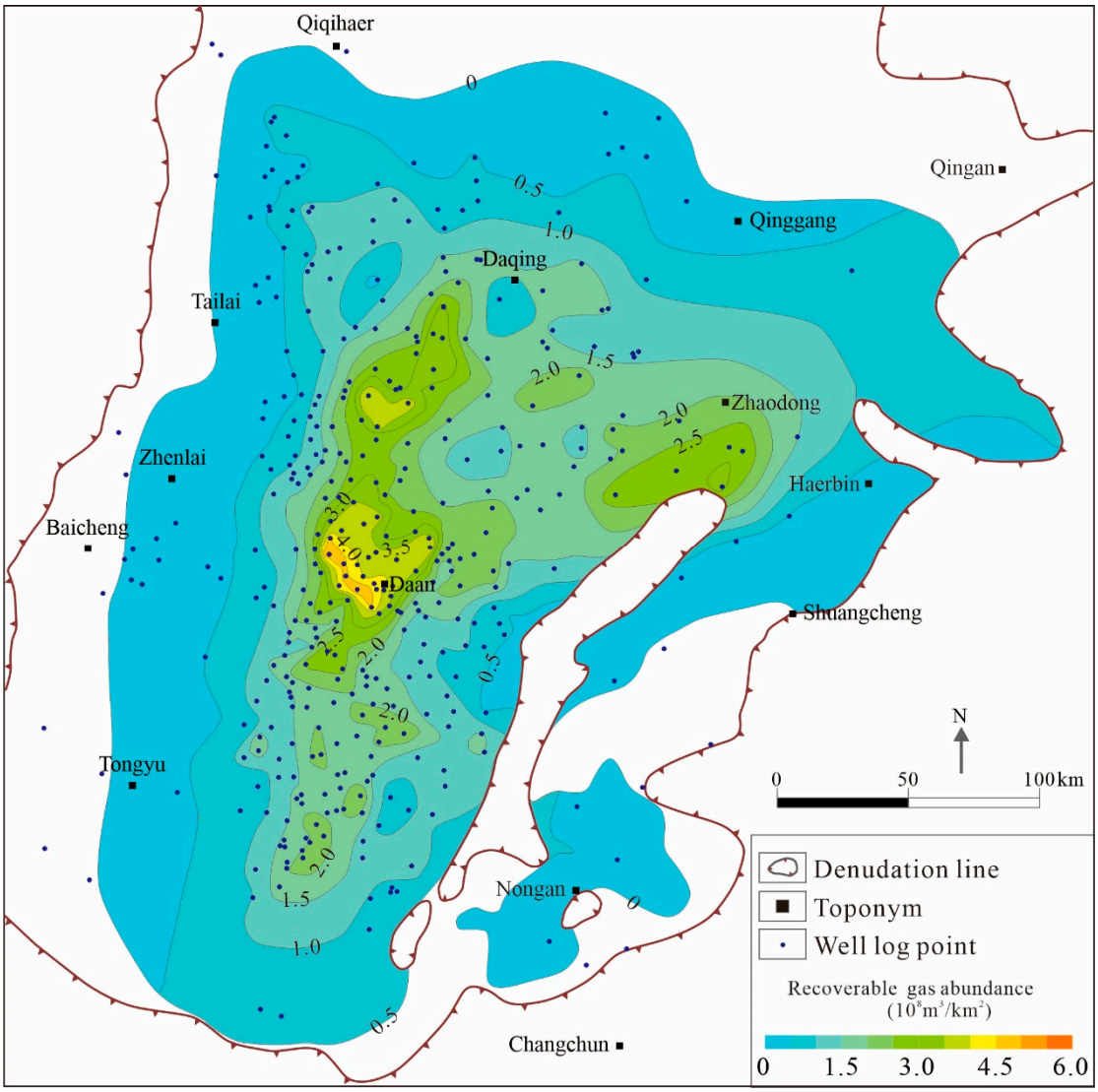

Figure 17. Abundance distribution of recoverable natural gas reserves in the bottom of Nenjiang Formation II.

 doi:10.20944/preprints202405.0272.v1

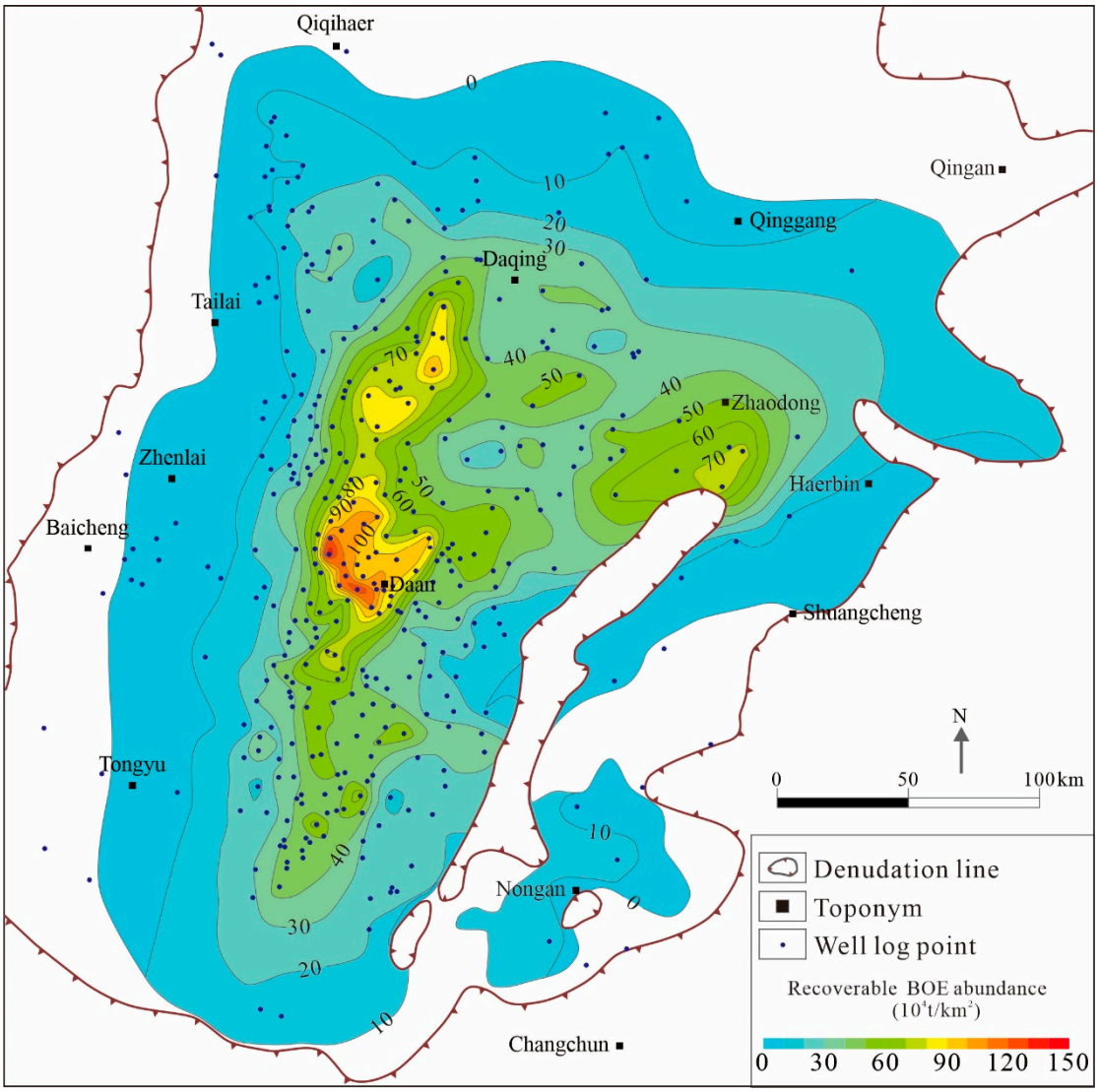

Figure 18. Abundance distribution of recoverable oil equivalent in the bottom of Nenjiang Formation II.

4. Conclusions

First, based on thermal simulation experiments on shale and crude oil samples for the purpose of in-situ conversion of organic matter in mature layers, it was found that the TOC, *Ro*, hydrocarbon generation potential, and fluid pressure would influence the hydrocarbon yield during in-situ conversion of the shale. Herein, the impact of liquid pressure and crude oil density on the final hydrocarbon yield per unit mass of residual oil can be considered as the foundation for establishing a model for hydrocarbon production via in-situ conversion of shale.

Second, following in-situ conversion thermal simulation experiments, a model for prediction of the amount of hydrocarbon produced from the solid organic matter in shale based on the TOC, *Ro*, fluid pressure, and hydrocarbon generation potential was established. Another model to estimate the amount of hydrocarbon production via in-situ conversion when residual hydrocarbons exist in the system, liquid pressure, and crude oil density was proposed. Moreover, in this study, we developed a method for determining key parameters for assessing the amount of recoverable hydrocarbon, which can be used to select favorable layers, especially in regions where in-situ conversion thermal simulation experiments have not been conducted.

Finally, based on the developed method the amount of recoverable hydrocarbon via in-situ conversion, was estimated in three zones of the Nenjiang Formation in the Songliao Basin to be

 doi:10.20944/preprints202405.0272.v1

approximately 292.02×10^8 t of oil and 18.58×10^{12} m^3 of natural gas. These results can provide a practical and theoretical basis for implementation of in-situ conversion operation in immature to low-maturity shale in the Nenjiang Formation and can serve as a guideline for the entire Songliao Basin, as well as universally around the globe on other shale formations where thermal simulation experiments have not been conducted.

Acknowledgments: We sincerely thank the Daqing Oilfield for data collection. This study is financially supported by the National Natural Science Foundation of China (Grant No. 42172170), and Prospective Fundamental Technology Research and Development Project of China National Petroleum Corporation (CNPC) (Grant No. 2021DJ52).

References

1. US Energy Information Administration. Short-term energy outlook. Washington: US Energy Information Administration, 2023.
2. Wang, X.; Zhang, G.; Tang, W.; Wang, D.; Wang, K.; Liu, J.; Du, D. A review of commercial development of continental shale oil in China. Energy Geoscience 2022, 3, 282-289.
3. Hu, T.; Pang, X.; Xu, T.; Li, C.; Jiang, S.; Wang, Q.; Chen, Y.; Zhang, H.; Huang, C.; Gong, S.; Gao, Z. Identifying the key source rocks in heterogeneous saline lacustrine shales: Paleogene shales in the Dongpu depression, Bohai Bay Basin, eastern China. AAPG Bulletin 2022, 106, 1325-1356.
4. Hou, L.; Luo, X.; Mi, J.; Zhang, Y.; Lin, S.; Liao, F.; Pang, Z. Characteristics of Oil and Gas Produced by In Situ Heating of Shale: A Case Study of the Chang 7 Member, Ordos Basin, China. Energy Fuels 2022, 36, 1429-1440.
5. Zhao, W.; Hu, S.; Hou, L.; Yang, T.; Li, X.; Guo, B.; Yang Z. Types and resource potential of continental shale oil in China and its boundary with tight oil. Petroleum Exploration and Development 2020, 47, 1-11.
6. Han, Z.; Wang, G.; Wu, H.; Feng, Z.; Tian, H.; Xie, Y.; Wu, H. Lithofacies Characteristics of Gulong Shale and Its Influence on Reservoir Physical Properties. Energies 2024, 17, 779.
7. Hu, T.; Pang, X.; Jiang, S.; Wang, Q.; Zheng, X.; Ding, X.; Zhao, Y.; Zhu, C.; Li, H. Oil content evaluation of lacustrine organic-rich shale with strong heterogeneity: A case study of the Middle Permian Lucaogou Formation in Jimusaer Sag, Junggar Basin, NW China. Fuel 2018, 221, 196-205.
8. Hou, L.; He, K.; Zhai, J.; Mi, J.; Weng, N. Compositional kinetics for hydrocarbon evolution in the pyrolysis of the Chang 7 organic matter: Implications for in-situ conversion of oil shale. Journal of Analytical and Applied Pyrolysis 2022, 162, 105434.
9. Liu, S.; Gai, H.; Cheng, P. Technical Scheme and Application Prospects of Oil Shale In Situ Conversion: A Review of Current Status. Energies 2023, 16, 4386.
10. Hou, L.; Ma, W.; Luo, X.; Liu, J. Characteristics and quantitative models for hydrocarbon generation-retention-production of shale under ICP conditions: example from the Chang 7 member in the Ordos Basin. Fuel 2020, 279, 118497.
11. Hu, T.; Liu, Y.; Jiang, F.; Pang, X.; Wang, Q.; Zhou, K.; Wu, G.; Jiang, Z.; Huang, L.; Jiang, S.; Zhang, C.; Li, M.; Chen, Z. A novel method for quantifying hydrocarbon micromigration in heterogeneous shale and the controlling mechanism. Energy 2024, 288, 129712.
12. Hou, L.; Luo, X.; Zhao, Z.; Zhang, L. Identification of Oil Produced from Shale and Tight Reservoirs in the Permian Lucaogou Shale Sequence, Jimsar Sag, Junggar Basin, NW China. ACS Omega 2021, 6, 2127-2142.
13. Ma, S.; Li, S.; Zhang, Z.; Xu, T.; Zheng, B.; Hu, Y.; Li, G.; Li, X. The Feasibility Study of In Situ Conversion of Oil Shale Based on Calcium-Oxide-Based Composite Materia Hydration Exothermic Reaction. Energies 2024, 17, 1798.
14. Zhao, Z.; Hou, L.; Luo, X.; Chi, Y.; Pang, Z.; Lin, S.; Zhang, L.; Liu, B. Heat-Induced Pore Structure Evolution in the Triassic Chang 7 Shale, Ordos Basin, China: Experimental Simulation of In Situ Conversion Process. Journal of Marine Science and Engineering 2023, 11, 1363.
15. Kang, Z.; Zhao, Y.; Yang, D. Review of oil shale in-situ conversion technology. Appl Energy 2020, 269, 115121.
16. Ma, W.; Hou, L.; Luo, X.; Liu, J.; Tao, S.; Guan, P.; Cai, Y. Generation and expulsion process of the Chang 7 oil shale in the Ordos Basin based on temperature-based semi-open pyrolysis: Implications for in-situ conversion process. Journal of Petroleum Science and Engineering 2020, 190, 107035.
17. Hou, L.; Cui, J.; Zhang, Y. Evolution mechanism of dynamic thermal parameters of shale. Marine and Petroleum Geology 2022, 138, 105423.
18. Hubbert, M. K. Degree of advancement of petroleum exploration in the United States. AAPG Bulletin 1967, 51, 2207-2227.
19. Burnham, A. K.; Mcconaghy, J. R. Comparison of the acceptability of various oil shale processes. In Proceedings of the 26th Oil Shale Symposium, Golden, CO, USA, 16–18 October 2006.

20. Fowler, T. D.; Vinegar, H. J. Oil shale ICP-Colorado Field Pilots. In Proceedings of the SPE Western Regional Meeting, San Jose, CA, USA, 24–26 March 2009; pp. 1–15.
21. Hou, L.; Luo, X.; Lin, S.; Li, Y.; Zhang, L.; Ma, W. Assessment of recoverable oil and gas resources by in-situ conversion of shale--Case study of extracting the Chang 7_3 shale in the Ordos Basin. Petroleum Science 2022, 19, 441-458.
22. Shen, Z.; Yu, Z.; Ye, H.; Deng, C.; He, H. Magnetostratigraphy of the Upper Cretaceous Nenjiang Formation in the Songliao Basin, northeast China: Implications for age constraints on terminating the Cretaceous Normal Superchron. Cretaceous Research 2022, 135, 105213.
23. Liu, B.; Wang, Y.; Tian, S.; Guo, Y.; Wang, L.; Yasin, Q.; Yang, J. Impact of thermal maturity on the diagenesis and porosity of lacustrine oil-prone shales: Insights from natural shale samples with thermal maturation in the oil generation window. International Journal of Coal Geology 2022, 261, 104079.
24. Wang, M.; Yang, J.; Wang, Z.; Lu, S. Nanometer-Scale Pore Characteristics of Lacustrine Shale, Songliao Basin, NE China. PLoS One 2015, 10, 0135252.
25. Wang, L.; Song, Z.; Yin, Q.; George, S. C. Paleosalinity significance of occurrence and distribution of methyltrimethyltridecyl chromans in the Upper Cretaceous Nenjiang Formation, Songliao Basin, China. Organic Geochemistry 2011, 42, 1411-1419.
26. Xu, J.; Liu, Z.; Bechtel, A.; Sachsenhofer, R. F.; Jia, J.; Meng, Q.; Sun, P. Organic matter accumulation in the Upper Cretaceous Qingshankou and Nenjiang Formations, Songliao Basin (NE China): Implications from high-resolution geochemical analysis. Marine and Petroleum Geology 2019, 102, 187-201.
27. Xu, Y.; Li, D.; Gao, Y.; Li, M.; Sun, L.; Zhang, X.; Wang, C.; Shen, Y. Multiple S-isotopic evidence for seawater incursions during the deposition of the upper Cretaceous source rocks in the Songliao Basin, northeastern China. Chemical Geology 2023, 642, 121790.
28. Chen, R.; Shang, F.; Cao, Y.; Song, L.; Li, Z. A comparative study of oil shale deposition in the Upper Cretaceous Nenjiang Formation, NE China: Evidence from petrographic and geochemical analyses. Journal of Petroleum Science and Engineering 2022, 219, 111130.
29. Shen, Z.; Yu, Z.; Ye, H.; Deng, C.; He, H. Magnetostratigraphy of the Upper Cretaceous Nenjiang Formation in the Songliao Basin, northeast China: Implications for age constraints on terminating the Cretaceous Normal Superchron. Cretaceous Research 2022, 135, 105213.
30. He, W.; Wang, M.; Wang, X.; Meng, Q.; Wu, Y.; Lin, T.; Li, J.; Zhang, J. Pore Structure Characteristics and Affecting Factors of Shale in the First Member of the Qingshankou Formation in the Gulong Sag, Songliao Basin. ACS Omega 2022, 7, 35755-35773.
31. Jia, J.; Bechtel, A.; Liu, Z.; Strobl, S. A.; Sun, P.; Sachsenhofer, R. F. Oil shale formation in the Upper Cretaceous Nenjiang Formation of the Songliao Basin (NE China): Implications from organic and inorganic geochemical analyses. International Journal of Coal Geology 2013, 113, 11-26.
32. Liu, B.; Liu, L.; Fu, J.; Lin, T.; He, J.; Liu, X.; Liu, Y.; Fu, X. The Songliao Super Basin in northeastern China. AAPG Bulletin 2023, 107, 1257–1297.
33. He, W.; Meng, Q.; Lin, T.; Wang, R.; Liu, X.; Ma, S.; Li, X.; Yang, F.; Sun, G. Evolution features of in-situ permeability of low-maturity shale with the increasing temperature, Cretaceous Nenjiang Formation, northern Songliao Basin, NE China. Petroleum Exploration and Development 2022, 49, 516-529.
34. Liu, W.; Liu, M.; Yang, T.; Liu, X.; Them, T. R.; Wang, K.; Bian C.; Meng, Q.; Li, Y.; Zeng, X.; Zhao, W. Organic matter accumulations in the Santonian-Campanian (Upper Cretaceous) lacustrine Nenjiang shale (K2n) in the Songliao Basin, NE China: Terrestrial responses to OAE3?, International Journal of Coal Geology 2022, 260, 104069.
35. Zhang, M.; Xie, R.; Yin, S.; Deng, M.; Chen, J.; Feng, S.; Luo, Z.; Chen, J. Logging identification of complex lithology of the Lower Jurassic Da'anzhai Member in the eastern slope of the western Sichuan Depression. Unconventional Resources 2023, 3, 7-19.